

1 Relationship of environmental relative humidity with North 2 Atlantic tropical cyclone intensity and intensification rate

3 Longtao Wu,^{1,2} Hui Su,¹ Robert G. Fovell,³ Bin Wang,⁴ Janice T. Shen,¹ Brian H. Kahn,¹
4 Svetla M. Hristova-Veleva,¹ Bjorn H. Lambriksen,¹ Eric J. Fetzer,¹ and Jonathan H. Jiang¹

5 Received 13 August 2012; revised 21 September 2012; accepted 23 September 2012; published XX Month 2012.

6 [1] Quantifying the relationship of large-scale environ-
7 mental conditions such as relative humidity with hurricane
8 intensity and intensity change is important for statistical
9 hurricane intensity forecasts. Our composite analysis of 9
10 years of Atmospheric Infrared Sounder (AIRS) humidity data
11 spanning 198 Atlantic tropical cyclones (TCs) shows that
12 environmental relative humidity (ERH) above the boundary
13 layer generally decreases with time as TCs evolve. Near the
14 surface, ERH stays approximately constant. ERH generally
15 increases with increasing TC intensity and intensification
16 rate. Rapidly intensifying TCs are associated with free tro-
17 pospheric ERH more than 10% (relative to the averaged ERH
18 for all TCs) larger than that for weakening TCs. Substantial
19 azimuthal asymmetry in ERH is also found, especially for the
20 TCs attaining the highest intensities and largest intensifica-
21 tion rates at distances greater than 400 km away from the TC
22 center. In the front-right quadrant relative to TC motion,
23 rapid intensification is associated with a sharp gradient of
24 ERH in the upper troposphere, with a decrease from the near
25 to the far environment between 400 hPa and 300 hPa. The
26 ERH gradient weakens with the decrease of intensification
27 rate. This radial ERH gradient might be a useful predictor for
28 the statistical forecast of TC intensification. **Citation:** Wu,
29 L., H. Su, R. G. Fovell, B. Wang, J. T. Shen, B. H. Kahn, S. M.
30 Hristova-Veleva, B. H. Lambriksen, E. J. Fetzer, and J. H. Jiang
31 (2012), Relationship of environmental relative humidity with
32 North Atlantic tropical cyclone intensity and intensification rate,
33 *Geophys. Res. Lett.*, 39, LXXXXX, doi:10.1029/2012GL053546.

34 1. Introduction

35 [2] While our understanding of tropical cyclones (TCs) has
36 improved tremendously in the past several decades, forecasts
37 of TC genesis, spin-up and subsequent (especially sudden)
38 intensity changes still present significant challenges. Official
39 intensity forecasts from the National Hurricane Center
40 (NHC) for Atlantic and Eastern North Pacific TCs have not
41 shown much improvement in the last 20 years [DeMaria

et al., 2007]. This is because TCs are sensitive to many fac-
tors, within the storm and in its surrounding environment.
For example, TC structure and intensity are sensitive to ver-
tical wind shear in the environment [DeMaria, 1996; Frank
and Ritchie, 2001; Zehr, 2003], which may be poorly fore-
casted by operational and research models. Also, relatively
subtle variations in sea-surface temperature (SST) or ocean
heat content can cause a TC intensity to shift several cate-
gories on the Saffir-Simpson scale within a short period of
time [Sun *et al.*, 2007].

[3] The available moisture of the TC's environment
represents another poorly understood influence on intensity,
thereby presenting a limit to predictability. While high mid-
tropospheric relative humidity (RH) appears to be necessary
for rapid intensification and the attainment of maximum
intensity [e.g., Kaplan and DeMaria, 2003; Emanuel *et al.*,
2004; Hendricks *et al.*, 2010; Kaplan *et al.*, 2010], dry air
intrusions have a negative influence on TC intensification as
dry air ingestion promotes the formation of cold downdrafts,
which transport low θ_e air into the sub-cloud layer and storm
inflow [e.g., Emanuel, 1989]. In an idealized modeling study,
Braun *et al.* [2012] showed that low humidity air reaching
the inner core induces asymmetric convective activity which
weakens TCs [e.g., Nolan and Grasso, 2003; Nolan *et al.*,
2007]. They further showed that the time for TCs to reach
maturity varies with the proximity of dry air to the center of
circulation. When dry air is located 270 km away or further
from the center of the vortex, its impact on TC intensity is
insignificant.

[4] Some studies [e.g., Barnes *et al.*, 1983; Wang, 2009]
have shown that substantial and extensive moisture may also
promote a net negative influence on TC strength by facilitat-
ing the formation of TC rainbands. The idealized modeling
study of Hill and Lackmann [2009], which varied the envi-
ronmental RH (ERH) in the region ≥ 100 km beyond the TC
core, suggests that larger ERH results in the establishment of
wider TCs with more prominent outer rainbands. However,
TC development, as measured by time series of maximum
10 m wind speeds, was nearly insensitive to ERH despite the
variation in rainband activity.

[5] Kaplan and DeMaria [2003] examined the mid-
tropospheric (850–700 hPa) ERH relation with rapidly
intensifying (RI) TCs in the North Atlantic basin using the
NHC HURDAT file [Jarvinen *et al.*, 1984] and the Statistical
Hurricane Intensity Prediction Scheme (SHIPS) [DeMaria
and Kaplan, 1999] database. Hendricks *et al.* [2010] con-
ducted composite analyses using the Navy Operational
Global Atmospheric Prediction System (NOGAPS) global
analysis. Both studies found that RI events over the Atlantic
basin are associated with larger RH in the middle troposphere
than non-RI events.

¹Jet Propulsion Laboratory, California Institute of Technology, Pasadena, California, USA.

²Joint Institute for Regional Earth System Science and Engineering, University of California, Los Angeles, California, USA.

³Department of Atmospheric and Oceanic Sciences, University of California, Los Angeles, California, USA.

⁴International Pacific Research Center, University of Hawaii at Manoa, Honolulu, Hawaii, USA.

Corresponding author: L. Wu, Jet Propulsion Laboratory, California Institute of Technology, 4800 Oak Grove Dr., M/S 183-701, Pasadena, CA 91109, USA. (longtao.wu@jpl.nasa.gov)

[6] Analyses using satellite observations have been rather limited. *Shu and Wu* [2009] examined the influence of the Saharan air layer (SAL) on TC intensity with three years of RH data from the Atmospheric Infrared Sounder (AIRS) instrument. They defined the SAL intrusion in the AIRS RH data as the nearest location of dry ($RH \leq 30\%$) air between 600 and 700 hPa. Their analysis incorporating 37 TCs during 2005–2007 suggested that the dry SAL air had a favorable influence on TC intensity when present in the northwest quadrant of TCs but a negative impact when the dry air approached to within 360 km, mostly in the southwest and southeast quadrants.

[7] In this study, we examine all TCs over the North Atlantic from 2002 to 2010. The RH analyses are stratified with respect to the radial distance from the TC center, altitude, maximum intensity attained by the TCs, and intensification rate. The primary goals of this study are to quantify the relationships between ERH and TC intensity and intensification rate, and improve our understanding of the impact of environmental moisture on TC development. In particular, the results of this study may help improve statistical models, which still show high skill in TC intensity forecasts when compared to advanced mesoscale numerical models [*Kaplan et al.*, 2010].

2. Data and Method

[8] The Atmospheric Infrared Sounder (AIRS) onboard the Aqua satellite since 2002 has provided near-daily global coverage of the tropospheric water vapor profile from space [*Divakarla et al.*, 2006; *Susskind et al.*, 2003]. The AIRS RH retrievals sample a broad ~ 1300 km swath at approximately 0130 and 1330 local time with a horizontal resolution of ~ 45 km near nadir. We use the Level 2 RH retrieval (version 5). The relative uncertainty of the RH retrieval is estimated to be 9% at 250 hPa and below, with no systematic bias [*Gettelman et al.*, 2006]. The six-hourly best track data for North Atlantic TCs are obtained from the Automated Tropical Cyclone Forecasting System (ATCF) at the NHC. This study summarizes the statistical behavior of 198 North Atlantic TCs, 74 of which achieved at least Category 1 intensity on the Saffir-Simpson scale, with a total of 2914 samplings observed by AIRS during the period of 2002 and 2010.

[9] Composites of ERH with respect to radial distance from the TC center, altitude, and quadrant with respect to TC motion are constructed. The TC center position at the local AIRS observational time is linearly interpolated from the best track data. Three zones of radial distances from the TC center are defined: the *near environment* (200–400 km), *intermediate environment* (400–600 km) and *far environment* (600–800 km). Using the best track data, four quadrants are established relative to TC motion in this study, numbered clockwise from the TC's front-right (Q1) to front-left sides (Q4). As TCs in the North Atlantic preferentially move westward, Q1 (Q4) roughly corresponds to the northwest (southwest) quadrant in geographic coordinate. There is a long tradition of using motion-based coordinates in composite construction [e.g., *George and Gray*, 1976], and motion itself contributes to storm asymmetry along with vertical wind shear and friction [e.g., *Corbosiero and Molinari*, 2003; *Chen et al.*, 2006; *DeMaria*, 1996; *Shapiro*,

1983] Future work will consider other coordinate systems, such as those based on vertical shear.

3. Results

3.1. Composite ERH as a Function of Time

[10] Each TC is examined for the ± 72 h period around its time of maximum intensity (T_{\max}). A composite temporal evolution of ERH is obtained by averaging ERH for each TC at the same time relative to T_{\max} . As shown in Figure 1, although individual measurements are quite scattered, the composite average ERH near surface (indicated by 1000–925 hPa layer) is about 82% for all four quadrants, with small variations throughout the 6-day period. ERH decreases with time at all altitudes above the boundary layer through the middle troposphere, and for all radial distances outward from the TC center. Furthermore, the magnitude of ERH declines from the near to the far environment. The average 500–600 hPa ERH in Q1 within the near environment is 56% at 72 h prior to peak intensity, dropping to 52% at T_{\max} and further diminishing to 37% by $T_{\max} + 72$ h. Over that same 6-day period, the far environment ERH at the same level declines from 42% to 36%. This ERH trend is possibly a result of TC-induced subsidence bringing down dry air from above that desiccates the lower and middle troposphere. Land influences could also play a role as TCs translate west- and northwest-ward. The physical factors contributing to the temporal drying effect warrant further investigation.

3.2. Composite ERH as a Function of TC Intensity

[11] The maximum wind speed (V_{\max}) from the best track data is used as an index for TC intensity and the ERH is then stratified with respect to TC intensity. Observed ERHs are normalized by the mean RH profile for the 198 TCs (see Figure S1 in the auxiliary material) and plotted as a function of V_{\max} for different radial distances from the TC center in Figure 2.¹

[12] In the near environment (Figure 2a), the TCs attaining the largest intensities (Category 5) possess a pronounced tendency towards having larger middle and upper tropospheric RH. This is seen in all quadrants and at all altitudes above the boundary layer. However, the changes of ERH with TC intensity are not linear. The correlation between the TC intensity and RH between 850 and 700 hPa (RH850) is 0.03 at Q1, but not statistically significant. The differences among TC categories are not always statistically significant. At radial distances exceeding 400 km from the TC center (Figures 2b and 2c), the composite ERH displays significant azimuthal asymmetry above the boundary layer. Relative to TC motion, the front quadrants (Q1 and Q4) have smaller mid-tropospheric RH while the rear quadrants (Q2 and Q3) have larger, especially in the far environment of Category 5 cases, where RH between 400 and 300 hPa (RH400) is 23% in Q1 and 51% in Q3.

3.3. Composite ERH as a Function of TC Intensification Rate

[13] The ERH is further stratified with respect to the TC intensification rate. The intensification rate at a particular time is defined as the V_{\max} difference between that time and

¹Auxiliary materials are available in the HTML. doi:10.1029/2012GL053546.

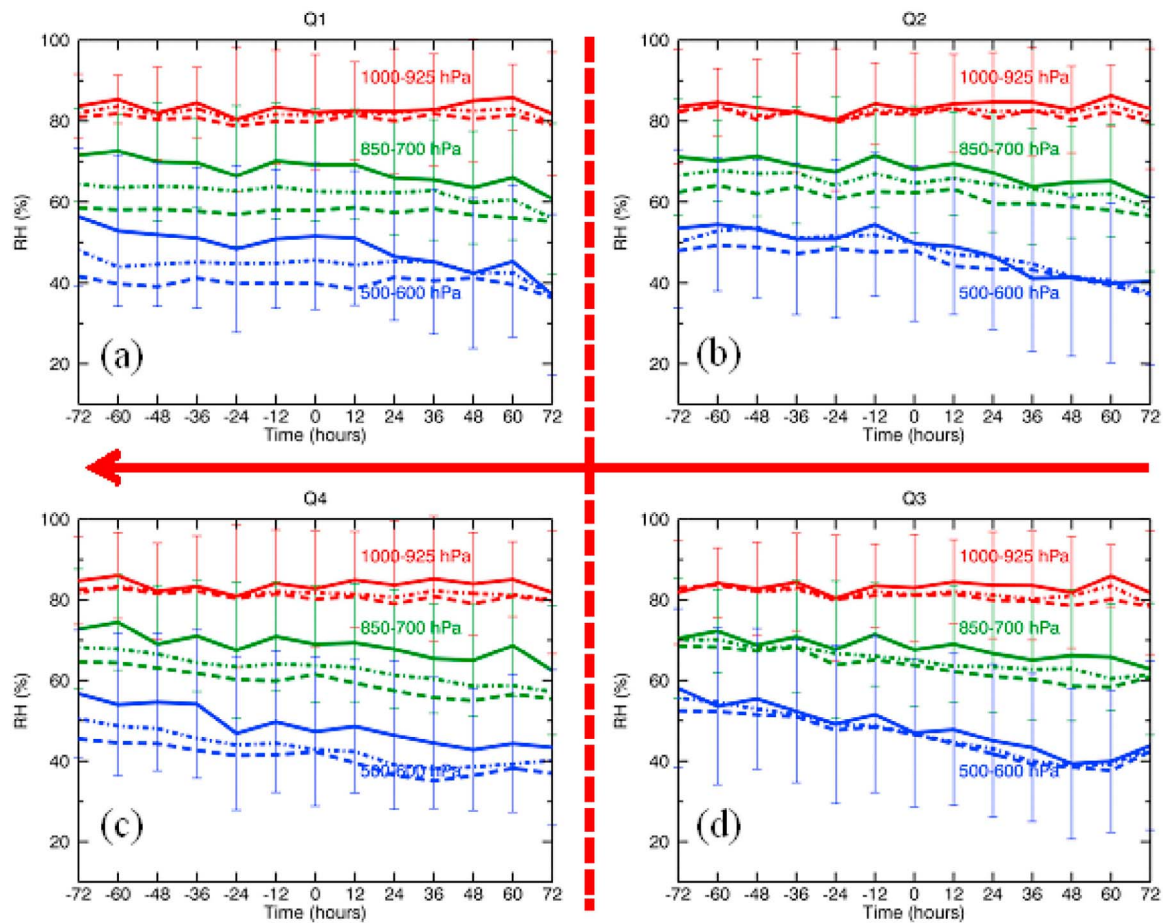


Figure 1. Time evolution of tropospheric RH at three pressure layers (1000–925 hPa in red; 850–700 hPa in green; 600–500 hPa in blue) averaged at three radial distances (near environment in solid line; intermediate environment in dash dot line; and far environment in dashed line), composited for 198 tropical cyclones over the North Atlantic Ocean from 2002 to 2010. Standard deviation is shown for near environment. The time “0” corresponds to the time of maximum TC intensity. (a) Quadrant 1 (Q1); (b) quadrant 2 (Q2); (c) quadrant 4 (Q4); (d) quadrant 3 (Q3). The red arrows indicate the preferential translation direction of TCs in the North Atlantic.

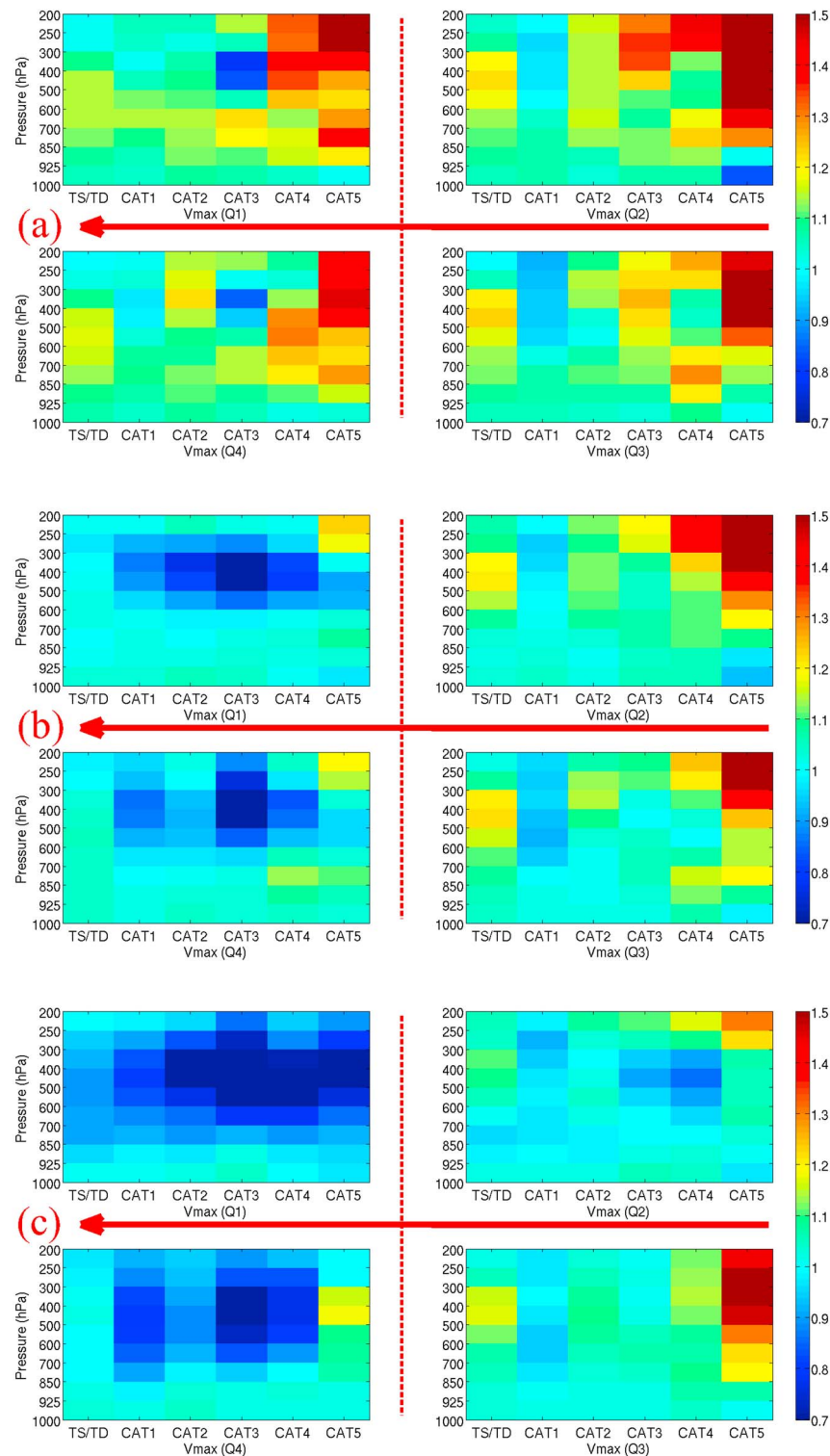


Figure 2. Normalized RH as a function of maximum TC intensity at three radial distances: (a) near environment; (b) intermediate environment; and (c) far environment. The normalization is with respect to the mean RH profile averaged for all 198 TC cases over the North Atlantic from 2002 to 2010 (see Figure S1). The four panels in each figure represent the four quadrants numbered from the front-right side of the TC (Q1) clockwise around to the front-left quadrant (Q4). The red arrows indicate the preferential translation direction of TCs in the North Atlantic.

Table 1. Averaged RH for Weakening (W: $-4.75 \leq \Delta V_{\max} < -0.75 \text{ m s}^{-1}$ per 6 hrs), Neutral (N: $-0.75 \leq \Delta V_{\max} < 2.25 \text{ m s}^{-1}$ per 6 hrs), Intensifying (I: $2.25 \leq \Delta V_{\max} < 4.75 \text{ m s}^{-1}$ per 6 hrs), Rapidly Intensifying (RI: $\Delta V_{\max} > 4.75 \text{ m s}^{-1}$ per 6 hrs) Cases, and the Differences Between RI and the Other Groups^a

Quantity	Mean	Quadrant	Distance	W	N	I	RI	RI – W	RI – N	RI – I	Corr
RH850 (850–700 hPa RH, %)	64.34	Q1	Near	64.55	68.18	71.84	71.90	7.35	3.72	0.06	0.15
			Intermediate	58.35	62.31	64.18	65.89	7.54	3.58	1.71	0.11
			Far	55.48	56.91	58.22	60.87	5.39	3.96	2.65	0.08
		Q3	Near	64.15	67.88	71.00	70.63	6.48	2.75	–0.07	0.15
			Intermediate	59.94	64.26	67.81	66.90	6.96	2.64	–0.91	0.16
			Far	58.33	62.60	66.82	66.36	8.03	3.74	–0.47	0.17
RH400 (400–300 hPa RH, %)	34.06	Q1	Near	<i>30.82</i>	<i>32.12</i>	<i>36.91</i>	<i>40.16</i>	9.34	8.04	3.25	0.09
			Intermediate	<i>31.94</i>	<i>31.77</i>	<i>32.04</i>	<i>31.25</i>	–0.69	–0.52	–0.79	–0.02
			Far	<i>32.43</i>	<i>31.50</i>	<i>29.26</i>	<i>27.45</i>	–4.98	–4.05	–1.71	–0.08
		Q3	Near	29.73	33.88	37.90	38.41	8.68	4.53	0.51	0.16
			Intermediate	28.75	33.58	37.57	40.35	11.60	6.77	2.78	0.16
			Far	28.96	33.11	37.19	38.87	9.91	5.76	1.69	0.17

^aIntensification rate (ΔV_{\max}) is defined as the 6-hour V_{\max} change. The sample size for each category is: 455 (W), 1592 (N), 500 (I) and 191 (RI). The second column is the mean value averaged for all 198 TC cases. The last column (Corr) is the correlation between the intensification rate and RH. The bold face denotes statistical significance at the 95% confidence level. The unique feature of RH400 in Q1 is italicized.

6 hours later. Five intensity change bins are defined: *rapidly intensifying* (RI), *intensifying* (I), *neutral* (N), *weakening* (W) and *rapidly weakening* (RW). RI (RW) corresponds to the top (bottom) 5% and the other three equally sample intensification rates for the 198 TCs. Following *Hendricks et al.* [2010], RW cases are not included in our discussions. The ranges of intensification rate and the sample sizes for each category are given in Table 1.

[14] Azimuthal asymmetry above the boundary layer in the intermediate and far environments is evident, in particular during RI (Figure 3). Similar to the composites with respect to intensity (Figure 2), Q2 and Q3 are generally more moist, while Q1 and Q4 are drier. However, correlations between ERH and intensification rate are quite low for all quadrants and environmental sectors (Table 1), which appears to be consistent with *Kaplan et al.* [2010], who found other environmental characteristics to be more skillful predictors of Atlantic basin RI. And yet, this is because simple linear relationships can obscure the potentially important variations discussed below.

[15] First, Table 1 and Figure 3 demonstrate that ERH tends to be positively associated with intensification rate, especially above the boundary layer in the near and intermediate environments. Storms undergoing RI possess larger than average ERH while weakening TCs are below the mean for the 198 TCs. As an example, for Q1 within the intermediate environment, RH between 850 and 700 hPa (RH850) is 58% while weakening, increasing to 62% at the neutral stage, both being below the overall average (64.3%; see Table 1). RH850 is about average (64%) during the intensifying stage and further increases to above average (66%) for RI.

[16] This means pairwise ERH differences between intensification categories can be sizable and significant. The 7.5% separating RI and W at 850 hPa is more than 10% above the averages for the two categories, as well as the overall mean, and exceeds the AIRS measurement uncertainty at this level. Like the other values listed with bold type in Table 1, this is significantly different from zero at the 95% level.

[17] At the 400 hPa level, the ERH differences in the near environment are even greater, and a *radial* variation in upper tropospheric humidity emerges in Q1, particularly during RI (Figure 3 and Table 1). RH400 in the near environment shifts from below (for W and N) to above average (for I and RI),

representing a RH change of about 9% (Table 1). Yet, for the far environment, the *lowest* ERH at this level is found at the RI stage for this quadrant, a decrease of 5% with respect to weakening TCs. It is striking that ERH actually *decreases* with intensification rate.

[18] Thus, as highlighted in Figure 4, the horizontal moisture *gradient* between the near and far environments in Q1 is largest during the RI stage, which is significant at the 99% level. This gradient is considerably smaller (but still statistically significant at the 90% level) during the intensifying stage, and of opposite sign for weakening cases. The RI stage's combination of larger and smaller ERH in the near and far environments, respectively, may reflect the influence of the storm-induced circulation or is possibly a controlling factor for TC intensification. This unique feature has not been documented before, and might yield a skillful predictor for statistical hurricane forecast models, potentially not less important than RH850 itself.

4. Conclusion and Discussion

[19] In this study, the ERH observed by AIRS is investigated in association with 198 TCs over the North Atlantic between 2002 and 2010. Composites of ERH with respect to radial distance from the TC center, altitude, and quadrant with respect to TC motion are constructed. The cases are also stratified with respect to time, TC intensity and intensification rate. The principal findings from this composite study of observational data are:

[20] 1. ERH in the free troposphere decreases with time as TCs evolve while ERH in the boundary layer stays approximately constant within ± 72 hours from the time that TCs reach maximum intensity. The ERH decrease in the free troposphere is possibly contributed by TC-induced subsidence and/or land influence.

[21] 2. Higher intensity TCs tend to have larger ERH than lower intensity TCs although the trend is not linear and not always statistically significant.

[22] 3. ERH above the boundary layer in the near environment generally increase with TC intensification rate. Rapidly intensifying TCs are associated with larger ERH than weakening and neutral TCs. However, the difference

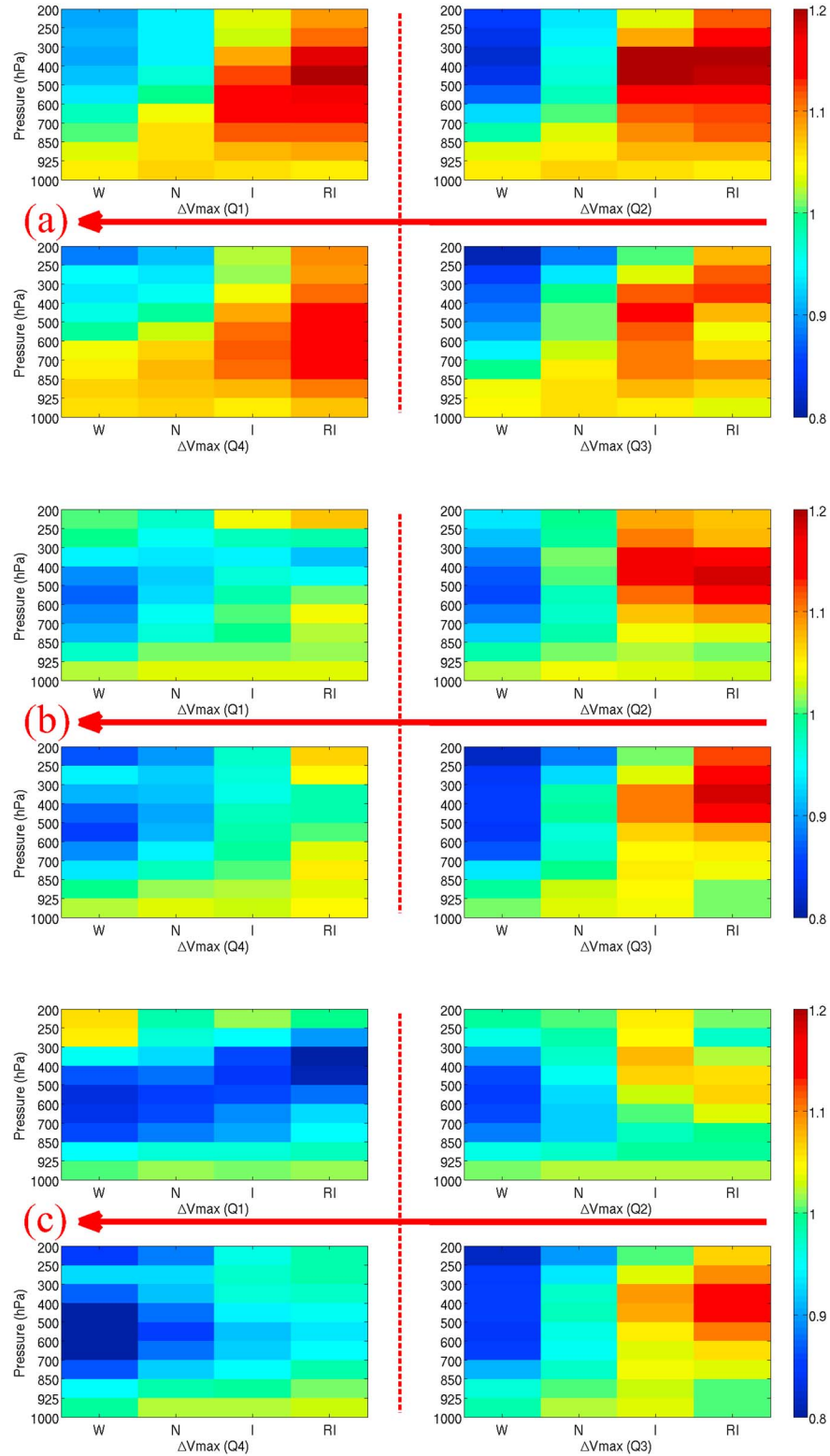


Figure 3. Normalized RH as a function of TC intensification rate at three radial distances: (a) near environment; (b) intermediate environment; and (c) far environment. The normalization is with respect to the mean RH profile averaged for all 198 TC cases over the North Atlantic from 2002 to 2010 (see Figure S1). The four panels represent the four quadrants numbered from the front-right side of the TC (Q1) clockwise around to the front-left quadrant (Q4). W: weakening ($-4.75 < \Delta V_{\max} < -0.75 \text{ m s}^{-1}$ per 6 hrs); N: neutral ($-0.75 < \Delta V_{\max} < 2.25 \text{ m s}^{-1}$ per 6 hrs); I: Intensifying ($2.25 < \Delta V_{\max} < 4.75 \text{ m s}^{-1}$ per 6 hrs); RI: rapidly intensifying ($\Delta V_{\max} > 4.75 \text{ m s}^{-1}$ per 6 hrs). The red arrows indicate the preferential translation direction of TCs in the North Atlantic.

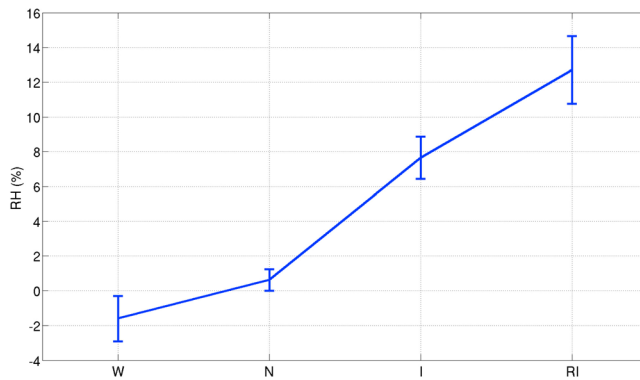


Figure 4. The averaged RH400 (RH between 400 and 300 hPa) difference between the near and far environments for each category in Q1. Vertical bars show the standard errors for each category.

300 between rapidly intensifying and intensifying cases are not
301 always statistically significant.

302 [23] 4. The azimuthal asymmetry of ERH becomes evident
303 at radial distances >400 km. The rear quadrants tend to have
304 larger ERH and the front quadrants appear to have lower
305 ERH.

306 [24] 5. In the front-right quadrant (Q1), a sharp decrease
307 in upper tropospheric (above 400 hPa) RH from the near to
308 the far environment occurs during rapid intensification. This
309 radial RH gradient is weaker for TCs with lower inten-
310 sification rates. For weakening TCs, Q1 has slightly larger
311 upper tropospheric ERH in the far environment than in the
312 near environment. This radial RH gradient may reflect the
313 influences of the storm-induced circulation or is possibly a
314 controlling factor for TC intensification. This radial RH
315 gradient might be a useful predictor for the forecast of TC
316 intensification.

317 [25] The AIRS-centric investigation provides new insights
318 regarding the environmental moisture within which TCs
319 grow, decay, and propagate. Our findings show a systematic
320 difference (on the order of several percent) between the
321 storms of different intensity or intensification rate. This sys-
322 tematic difference represents a signal that cannot be simply
323 dismissed via limitations inherent in the measurements. The
324 relationship of ERH with TC intensity and intensification
325 rate, especially its azimuthal and radial variations, may lead to
326 improvements in TC intensity forecasts from statistical models.

327 [26] There are remaining questions that warrant further
328 investigation, particularly in regards to whether the observed
329 relationships represent the impact of ERH on TC develop-
330 ment, or a more complex set of nonlinear interactions
331 between a TC and its environment. For example, is the dry
332 air in the front-right quadrant in the intermediate and far
333 environments providing a favorable (by suppressing rain-
334 band convection) or detrimental influence on TC intensifi-
335 cation? Or, is it simply a result of the TC circulation (from
336 subsidence drying)? Additional numerical model experi-
337 ments could help clarify the role of environmental moisture
338 in TC evolution. This observational analysis will be valuable
339 for the validation of numerical and statistical models.

340 [27] **Acknowledgments.** The authors thank Sundararaman
341 Gopalakrishnan and Tomislava Vukicevic for valuable discussions, and
342 Mark DeMaria for suggestions. The helpful comments from two anonymous

reviewers are appreciated. The work is conducted at the Jet Propulsion
Laboratory, California Institute of Technology, under contract with NASA.
The authors thank the funding support from the NASA HSRP program.
[28] The Editor thanks the two anonymous reviewers for their assistance
in evaluating this paper.

References

- Barnes, G. M., E. J. Zipser, D. Jorgensen, and F. Marks Jr. (1983), Mesoscale and convective structure of a hurricane rainband, *J. Atmos. Sci.*, **40**, 2125–2137, doi:10.1175/1520-0469(1983)040<2125:MACSOA>2.0.CO;2.
- Braun, S. A., J. A. Sippel, and D. S. Nolan (2012), The impact of dry mid-level air on hurricane intensity in idealized simulations with no mean flow, *J. Atmos. Sci.*, **69**, 236–257, doi:10.1175/JAS-D-10-05007.1.
- Chen, S. S., J. A. Knaff, and F. D. Marks Jr. (2006), Effects of vertical wind shear and storm motion on tropical cyclone rainfall asymmetries deduced from TRMM, *Mon. Weather Rev.*, **134**, 3190–3208, doi:10.1175/MWR3245.1.
- Corbosiero, K. L., and J. Molinari (2003), The relationship between storm motion, vertical wind shear, and convective asymmetries in tropical cyclones, *J. Atmos. Sci.*, **60**, 366–376, doi:10.1175/1520-0469(2003)060<0366:TRBSMV>2.0.CO;2.
- DeMaria, M. (1996), The effect of vertical shear on tropical cyclone intensity change, *J. Atmos. Sci.*, **53**, 2076–2088, doi:10.1175/1520-0469(1996)053<2076:TEOVSO>2.0.CO;2.
- DeMaria, M., and J. Kaplan (1999), An updated Statistical Hurricane Intensity Prediction Scheme (SHIPS) for the Atlantic and eastern North Pacific Basins, *Weather Forecast.*, **14**, 326–337, doi:10.1175/1520-0434(1999)014<0326:AUSHIP>2.0.CO;2.
- DeMaria, M., J. A. Knaff, and C. Sampson (2007), Evaluation of long-term trends in tropical cyclone intensity forecasts, *Meteorol. Atmos. Phys.*, **97**, 19–28, doi:10.1007/s00703-006-0241-4.
- Divakarla, M. G., C. D. Barnet, M. D. Goldberg, L. M. McMillin, E. Maddy, W. Wolf, L. Zhou, and X. Liu (2006), Validation of Atmospheric Infrared Sounder temperature and water vapor retrievals with matched radiosonde measurements and forecasts, *J. Geophys. Res.*, **111**, D09S15, doi:10.1029/2005JD006116.
- Emanuel, K. A. (1989), Dynamical theories of tropical convection, *Aust. Meteorol. Mag.*, **37**, 3–10.
- Emanuel, K., C. DesAutels, C. Holloway, and R. Korty (2004), Environmental control of tropical cyclone intensity, *J. Atmos. Sci.*, **61**, 843–858, doi:10.1175/1520-0469(2004)061<0843:ECOTCI>2.0.CO;2.
- Frank, W. M., and E. A. Ritchie (2001), Effects of vertical wind shear on the intensity and structure of numerically simulated hurricanes, *Mon. Weather Rev.*, **129**, 2249–2269, doi:10.1175/1520-0493(2001)129<2249:EOVWSO>2.0.CO;2.
- George, J. E., and W. M. Gray (1976), Tropical cyclone motion and surrounding parameter relationships, *J. Appl. Meteorol.*, **15**, 1252–1264, doi:10.1175/1520-0450(1976)015<1252:TCMASP>2.0.CO;2.
- Gottelman, A., E. J. Fetzer, A. Eldering, and F. W. Irion (2006), The global distribution of supersaturation in the upper troposphere from the Atmospheric Infrared Sounder, *J. Clim.*, **19**, 6089–6103, doi:10.1175/JCLI3955.1.
- Hendricks, E. A., M. S. Peng, B. Fu, and T. Li (2010), Quantifying environmental control on tropical cyclone intensity change, *Mon. Weather Rev.*, **138**, 3243–3271, doi:10.1175/2010MWR3185.1.
- Hill, K. A., and G. M. Lackmann (2009), Influence of environmental humidity on tropical cyclone size, *Mon. Weather Rev.*, **137**, 3294–3315, doi:10.1175/2009MWR2679.1.
- Jarvinen, B. R., C. J. Neumann, and M. A. S. Davis (1984), A tropical cyclone data tape for the North Atlantic basin, 1886–1983: Contents, limitations, and uses, *NOAA Tech. Memo. NWS NHC 22*, 21 pp., Natl. Weather Serv., Miami, Fla.
- Kaplan, J., and M. DeMaria (2003), Large-scale characteristics of rapidly intensifying tropical cyclones in the North Atlantic basin, *Weather Forecast.*, **18**(6), 1093–1108, doi:10.1175/1520-0434(2003)018<1093:LCORIT>2.0.CO;2.
- Kaplan, J., M. DeMaria, and J. A. Knaff (2010), A revised Tropical Cyclone Rapid Intensification Index for the Atlantic and eastern North Pacific Basins, *Weather Forecast.*, **25**, 220–241, doi:10.1175/2009WAF2222280.1.
- Nolan, D. S., and L. D. Grasso (2003), Nonhydrostatic, three-dimensional perturbations to balanced, hurricane-like vortices. Part II: Symmetric response and nonlinear simulations, *J. Atmos. Sci.*, **60**, 2717–2745, doi:10.1175/1520-0469(2003)060<2717:NTPTBH>2.0.CO;2.
- Nolan, D. S., Y. Moon, and D. P. Stern (2007), Tropical cyclone intensification from asymmetric convection: Energetics and efficiency, *J. Atmos. Sci.*, **64**, 3377–3405, doi:10.1175/JAS3988.1.
- Shapiro, L. J. (1983), The asymmetric boundary layer flow under a translating hurricane, *J. Atmos. Sci.*, **40**, 1984–1998, doi:10.1175/1520-0469(1983)040<1984:TABLFU>2.0.CO;2.

- 421 Shu, S., and L. Wu (2009), Analysis of the influence of Saharan air layer on
422 tropical cyclone intensity using AIRS/Aqua data, *Geophys. Res. Lett.*, *36*,
423 L09809, doi:10.1029/2009GL037634. 429
- 424 Sun, D. L., M. Kafatos, G. Cervone, Z. Boybeyi, and R. X. Yang (2007),
425 Satellite microwave detected SST anomalies and hurricane intensifica- 430
426 tion, *Nat. Hazards*, *43*(2), 273–284, doi:10.1007/s11069-006-9099-5. 431
- 427 Susskind, J., C. D. Barnett, and J. Blaisdell (2003), Retrieval of atmospheric 432
428 and surface parameters from AIRS/AMSU/HSB data under cloudy 433
conditions, *IEEE Trans. Geosci. Remote Sens.*, *41*(2), 390–409, 434
doi:10.1109/TGRS.2002.808236. 435
- Wang, Y. (2009), How do outer spiral rainbands affect tropical cyclone 436
structure and intensity?, *J. Atmos. Sci.*, *66*, 1250–1273, doi:10.1175/
2008JAS2737.1.
- Zehr, R. M. (2003), Environmental vertical wind shear with Hurricane Ber-
tha (1996), *Weather Forecast.*, *18*, 345–356, doi:10.1175/1520-0434
(2003)018<0345:EVWSWH>2.0.CO;2.

Article in Proof